Electrochemically Induced Conformational Changes in Cytochrome *c* Monitored by Fourier Transform Infrared Difference Spectroscopy: Influence of Temperature, pH, and Electrode Surfaces†

Daniela D. Schlereth and Werner Mäntele*

Institut für Biophysik, Albertstrasse 23, D-7800 Freiburg, Germany

Received June 11, 1992; Revised Manuscript Received September 1, 1992

ABSTRACT: IR difference spectra between the oxidized and the reduced state of horse heart cytochrome *c* were obtained for different temperature and pH conditions at various surface-modified electrodes using an optically transparent thin-layer electrochemical cell. These difference spectra reflect changes in protein conformation, side-chain geometries, and protonation upon the redox transition. The IR difference spectra recorded in the 10–40 °C temperature range showed thermally induced changes mainly in the amide-I (1700–1600 cm^{-1}) and in the amide-II (ca. 1550 cm^{-1}) spectral regions. Although the position of most of the signals remains unshifted, large differences in their relative amplitude were observed, leading in some cases to the masking and/or the disappearance of some IR signals. In the range 6.8–9.8, increasing pH of the samples led to a decrease in the reduction rate and to spectral changes which closely resemble those obtained by increasing the temperature. Both the thermal and the pH dependence of the reduced-minus-oxidized IR difference spectra reflect the transition of ferricytochrome *c* from the native to the alkaline form. An analysis of the IR difference spectra shows that the redox transition at neutral pH involves mainly β-turns and β-sheet segments of the cytochrome *c* molecule. However, once the ferricytochrome *c* alkaline transition is performed, the redox process is coupled to conformational changes involving α-helical segments. The shifts in tyrosine vibrational modes observed in the difference spectra obtained at neutral and slightly alkaline pH at high temperatures suggest an intermediate state of the ferricytochrome *c* in which the heme crevice is more accessible to the solvent. We propose that the influence of the electrode surface on the spectral changes observed may arise from the different nature of the interaction between the protein and the promoter molecules adsorbed on the electrode surface. The strength of this interaction plays an important role in the stabilization of the native structure of cytochrome *c* and thus delays the process of the loosening of the structure of the heme crevice. Either a metallic surface which is not fully covered or an excess of negative charges on the electrode surface may favor an opened or partially unfolded conformation of the protein.

For their physiological function as electron carriers in the electron transport chain, it has been suggested that the electron transfer between the *c*-type cytochromes and their oxidoreductases is facilitated by electrostatic interactions involving a belt of positive charges formed by conserved lysine residues surrounding the exposed heme crevice (Salemme et al., 1973). Hypothetical three-dimensional models of cytochrome *c* complexes with cytochrome b_5 (Salemme, 1976) and cytochrome-*c* peroxidase (Poulos & Kraut, 1980) suggest that in these complexes the proteins are held together by optimizing hydrogen-bonding interactions between complementary charged groups. Both proteins are arranged in a spatial configuration in which both heme groups are parallel.

Crystallographic data from tuna and yeast iso-1-cytochrome *c* in both oxidation states reveal that the redox process is coupled to concerted small conformational changes which are more obvious in the bottom half of the molecule and in the Met-80 side of the heme (Takano & Dickerson, 1981a,b; Berghuis & Brayer, 1992). After the redox transition, all the main-chain hydrogen-bond interactions are retained, and the movements in the molecule could be described as adjustments to the heme structure, large movements of the internally bound water molecules, and segmental thermal parameter changes along the polypeptide chain (Berghuis & Brayer, 1992).

However, there are some discrepancies among data obtained from different spectroscopic techniques which give information about the structural changes exhibited by the protein upon the redox transition in solution.

Whereas the differences in the NMR chemical shifts observed between both oxidation states suggest a very small conformational change in the same line as in the crystalline state (Feng et al., 1990), the UV resonance Raman spectra suggest a larger conformational change with alterations in the tertiary contacts depending on the redox state (Liu et al., 1989).

In a recent paper, we have analyzed the reduced-minus-oxodized (red-ox)[1] infrared difference spectrum of cytochrome *c* (Moss et al., 1990). The difference spectrum was obtained by electrochemical reduction/oxidation of the redox protein in a spectroelectrochemical cell designed for IR (and UV–vis) spectroscopy.

This combination of electrochemical techniques with the extreme sensitivity of Fourier transform infrared (FTIR)

† D.D.S. gratefully acknowledges a post-doctoral fellowship from the spanish Consejo Superior de Investigaciones Cientfficas. W.M. is indebted to the Deutsche Forschungsgemeinschaft for financial support (Ma 1054/2-2 and 5-1) and a Heisenberg fellowship.

[1] Abbreviations: PyS, bis(4-pyridyl)disulfide; Cys, cysteine; HPrS, 3,3′-dithiodipropionic acid; MB, methylene blue; hh cyt *c*, horse heart cytochrome *c*; red-ox, reduced-minus-oxidized; OTTLE cell; optically transparent thin-layer electrochemical cell; T_{tr}, transition temperature; SME, surface-modified electrodes.

0006-2960/93/0432-1118$04.00/0

spectroscopy, which is a consequent development of previous reaction-modulated IR difference techniques for the large class of redox proteins, allowed us to detect the contributions of individual bonds to the absorbance spectrum of the entire protein.

The reduced-minus-oxidized FTIR difference spectra of different cytochromes c from different species show that indeed there must be a movement of the polypeptide backbone upon the redox transition and suggest that the conformational change must be essentially the same for several species of mammalian cytochromes c (Moss et al., 1990).

Large differences in the secondary structure content between both oxidation states have also been found from the second-derivative amide-I IR spectra of horse heart cytochrome c (hh cyt c), involving mostly β-turn 3_{10} and β-sheet segments (Dong et al., 1992).

A characteristic feature of cyt c is the dependence of its formal redox potential on several parameters such as temperature, pH, ionic strength, type of electrolyte, and type of buffer. There is a shift toward more negative potentials with the increase of temperature and pH. The temperature dependence shows a sharp biphasic behavior which has been explained on the basis of the existence of a conformational change between two states of ferricytochrome c, with an apparent pK_a = 9.8 at 20 °C. This thermal transition is reversible and accelerated with the pH increase (Ikeshoji et al., 1989).

A decrease of the formal redox potential is related with a heme crevice more exposed to the solvent (Stellwagen, 1978). Stable "opened" conformers of hh cyt c have been described with a formal potential 500 mV lower than the native conformation (Hinnen & Niki, 1989; Hildebrandt & Stockburger; 1989a; Santucci et al., 1989).

A stable opened conformation of cyt c is induced by low ionic strength (Liu et al., 1989; Feng et al., 1990), partial denaturation with 4.5 M urea (Myer et al., 1980), or temperature increase (Angström et al., 1982), or by electrostatic interactions with negatively charged phospholipid membranes (Muga et al., 1991), vesicles and micellar systems (Hildebrandt & Stockburger, 1989b), or metallic surfaces (Hildebrandt & Stockburger, 1986, 1989a).

The "opened" conformation may exhibit changes in the coordination shell induced by electrostatic interactions (Hildebrandt & Stockburger, 1989a,b). In an earlier work, Myer et al. (1980) suggested that the decrease of the pK_a of the alkaline transition from 9.2 to 8.5 in the partially denaturated form of hh cyt c with 4.5 M urea reflects a destabilization of the protein not only in terms of polypeptide conformation but also with respect to the coordination configuration of the heme iron.

On the other hand, Angström et al. (1982) showed that at neutral pH there is a thermally induced transition to the low-spin alkaline form of ferricytochrome c at 40 °C. At pH 5.4, however, the thermal transition gives rise to a high-spin species resulting from the rupture of the Fe(III)–S(Met-80) bond. Cyt c adsorbed in colloidal silver particles shows at temperatures below 22 °C an adsorption-induced partial transition from the low-spin state to the high-spin state (Hildebrandt & Stockburger, 1986).

In this work we show the reduced-minus-oxidized (red-ox) IR difference spectra of both neutral and alkaline forms of hh cyt c. Both thermal and pH-induced processes lead to the transition from the neutral to the alkaline form of the spectra, thus reflecting the same conformational transition. The conditions at which the alkaline transition is reached depend on the electrode surface. This demonstrates that the interaction between the protein and the different promoters adsorbed on the electrode surface is specific for each promoter. Thus, the nature of the surface modifiers seems to be an essential parameter to be taken into account in this kind of spectroelectrochemical studies.

MATERIALS AND METHODS

Sample Preparation. The OTTLE cell sutiable for UV–VIS and IR spectroscopy of proteins in aqueous solvents has been described previously (Moss et al., 1990) and used with minor modifications (Baymann et al., 1991). As an essential feature of this cell, the protein solution forms a 10–15-μm layer on a 70% transparent gold grid working electrode (Buckbee-Mears, St. Paul, MN) between two calcium fluoride windows, in electrical contact with a platinum foil counter electrode and a Ag/AgCl/3 M KCl reference electrode (all the potentials quoted in this work are referrred to this electrode, add +208 mV for potentials vs Standard Hydrogen Electrode).

Horse heart cytochrome c (type VI) was purchased from Sigma and used without further purification. The samples were prepared at concentrations between 5 and 15 mM in 50 mM phosphate buffer containing 100 mM $LiClO_4$ as a supporting electrolyte. For measurements at pH 9.8, a little amount of KOH was added to a 50 mM K_2PO_4H–100 mM $LiClO_4$ buffer.

The gold grid working electrode was freshly modified before each experiment, following the procedures described below, and rinsed thoroughly with distilled water to avoid the presence of the modifier in the protein solution. Filling of the cell was performed according the procedure described by Moss et al. (1990).

Gold Grid Modification. Bis(4-pyridyl)disulfide electrodes (PyS-SMEs) (Sigma) were prepared by soaking the grid for 10 min with a 0.8 mg/mL acidic solution of the compound as described by Taniguchi et al. (1982a,b).

Cysteine electrodes (Cys-SMEs) (Sigma) were prepared by soaking the grid for 10 min with a 10 mg/mL aqueous solution of L-cysteine as described by Di Gleria et al. (1986).

3,3′-Dithiodipropionic acid electrodes (HPrS-SMEs) (Fluka) were prepared by cyclic scanning of a 1 mM HPrS solution between 0 and −950 mV as described by Hill and Lawrance (1989).

Methylene blue electrodes (MB–SMEs) (Sigma) were prepared by cyclic scanning of a 1 mM MB solution between +500 and −600 mV as described previously (Schlereth & Mäntele, 1992).

FTIR Difference Spectroscopy. For the acquisition of a reduced-minus-oxidized (red-ox) IR difference spectrum, a 5 mM hh cyt c sample was first equilibrated at +300 mV for 100 s (+500 mV for MB electrodes) in order to fully oxidize the sample. After that, an IR single-beam spectrum of the oxidized state was recorded as a reference. A reducing potential of −300 mV (−500 mV for MB electrodes) was then applied for 100 s, and the IR spectrum of the reduced state was recorded. The oxidation/reduction process of the sample was monitored by the absorbance change at 550 nm.

Each single-beam spectrum was the average of 32 scans at 3 scans/s on a Bruker IFS 25 FTIR spectrophotometer equipped with a MCT detector of selected sensitivity. The FTIR spectrophotometer was modified in order to allow the measuring beam of the single-beam spectrophotometer for visible light to pass coaxially through the sample, thus allowing simultaneous recording of the UV–VIS and IR spectra. The difference spectra were calculated from single-beam spectra (I_1,I_2) of the sample equilibrated at the different potentials by forming $A = \log (I_2/I_1)$. All the spectra shown in this

work are the result of the average of several spectra recorded after successive electrochemical cycles. No baseline subtractions or weighted subtractions of buffers were performed. Both spectroscopy and electrochemistry were controlled through interfaces from a data acquisition and treatment software ("MSPEK") developed in our laboratory by D. Moss and S. Grzybek. The temperature was controlled by a thermostat in the range between 10 and 40 °C.

RESULTS

The electrochemically induced red-ox IR difference spectrum of hh cyt *c* at neutral pH and room temperature has been previously published (Moss et al., 1990). In this previous work much effort was devoted to assign signals arising from specific amino acids which are thought to be actively involved in the redox transition, stabilization of a redox state, and interactions with the redox partners. In addition, it was shown with a redox titration that all bands titrate in unison and are fully reversible, and that even minor bands can be reliably attributed to the cytochrome *c* redox process.

However, a comparison between this red-ox difference spectrum and the amide-I IR second-derivative absorbance spectra of chemically reduced and oxidized hh cyt *c* (Dong et al., 1990, 1992) shows that the electrochemically induced IR difference spectrum can also give valuable information about the changes in the secondary structure produced upon the redox transition.

Reduced-Minus-Oxidized IR Difference Spectrum of Horse Heart Cytochrome c at Neutral pH and Low Temperature. In order to get the IR red-ox difference spectra, the electrochemical reaction was monitored by the time-dependent absorbance change at 550 nm after the application of a potential step. Figure 1, parts A and B, shows the visible difference spectrum and the electrolysis rates of oxidation and reduction of hh cyt *c* at the different surface-modified electrodes at pH 6.8 and 30 °C.

Figure 2, parts a, b, and c, shows the red-ox IR difference spectrum of hh cyt *c* at different pHs in the range 6.8–9.8 obtained with the PyS-SME. For each pH, a series of spectra recorded at different temperatures in the range 10–40 °C is also shown.

Figure 2a (thick line) shows the spectrum at pH 6.8 recorded at 10 °C. The signals of higher amplitude appear in the amide-I region (1700–1600 cm^{-1}) at 1692(+), 1672(–), 1662-(+), 1650(–), 1634(–), 1626(+); and 1612(–) cm^{-1}. The positions of all these signals agree with those obtained from the amide-I IR second-derivative spectrum by Dong et al. (1990, 1992), where they have been assigned to C=O stretching modes of peptides belonging to different secondary structures. The sum of the amplitudes of these difference signals corresponds at most to 10% of the amide-I band amplitude obtained in the absolute IR spectrum. From these data we can conclude that there are only very few (at the most 10) amino acids involved in the conformational change produced upon the redox transition. From the analysis of the amide-I IR second-derivative spectra of both oxidation states of hh cyt *c*, it was found that between 9 and 13 amino acids were involved in the redox conformational change (Dong et al., 1992).

Among the difference bands in the 1700–1600 cm^{-1} spectral region, Moss et al., (1990) have assigned the 1692(+) cm^{-1} signal to the symmetric stretching mode of COOH of a protonated heme propionic acid. We consider here the possibility of an additional contribution from the C=O stretching mode of peptides included in β-turn segments (Susi

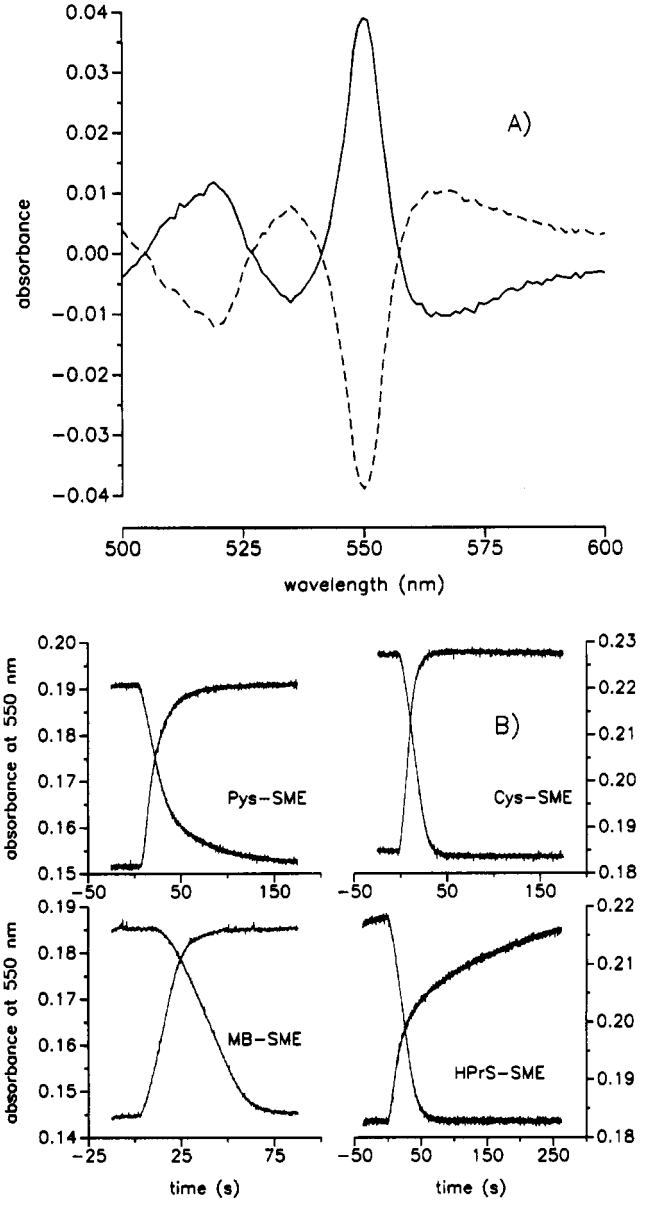

FIGURE 1: (A) Red-ox visible difference spectrum of hh cyt *c* in the α-band region. (B) Time-dependent absorbance change at 550 nm at the different SMEs at pH 6.8, 30 °C. Electrolysis cycles +300/−300 mV (+500/−500 mV for MB-SMEs).

& Byler, 1987; Surewicz et al., 1987; Arrondo et al., 1988). In this line, the 1672(–) cm^{-1} signal may be attributed to parallel β-strands (Krimm & Bandekar, 1986; Surewicz et al., 1987; Arrondo et al., 1988). A band in the second-derivative spectra of Dong et al. (1992) at 1650 cm^{-1} has been assigned to random coil structures, an interpretation which may also be possible for the negative 1650 cm^{-1} difference band in Figure 2a and in the spectra obtained by Moss et al. (1990). However, it may also include a contribution of β-turns (II) (Krimm & Bandekar, 1986).

For the signals at 1634(–) and 1626(+) cm^{-1}, an interpretation in terms of antiparallel chain pleated β-sheet structures (Krimm et al., 1986) and of exposed β-strands (Casal et al., 1988; Arrondo et al., 1988), respectively, appears possible. At the lower end of the amide-I absorbance range, contributions from an antiparallel β-sheet appear a possible explanation for the 1612 cm^{-1} band (Wantyghem et al., 1990). However, in this region the HC=CH stretching mode of side-chain aromatic rings should also appear (Surewicz et al., 1987). Liu et al. (1989) have assigned in the Raman spectrum of hh

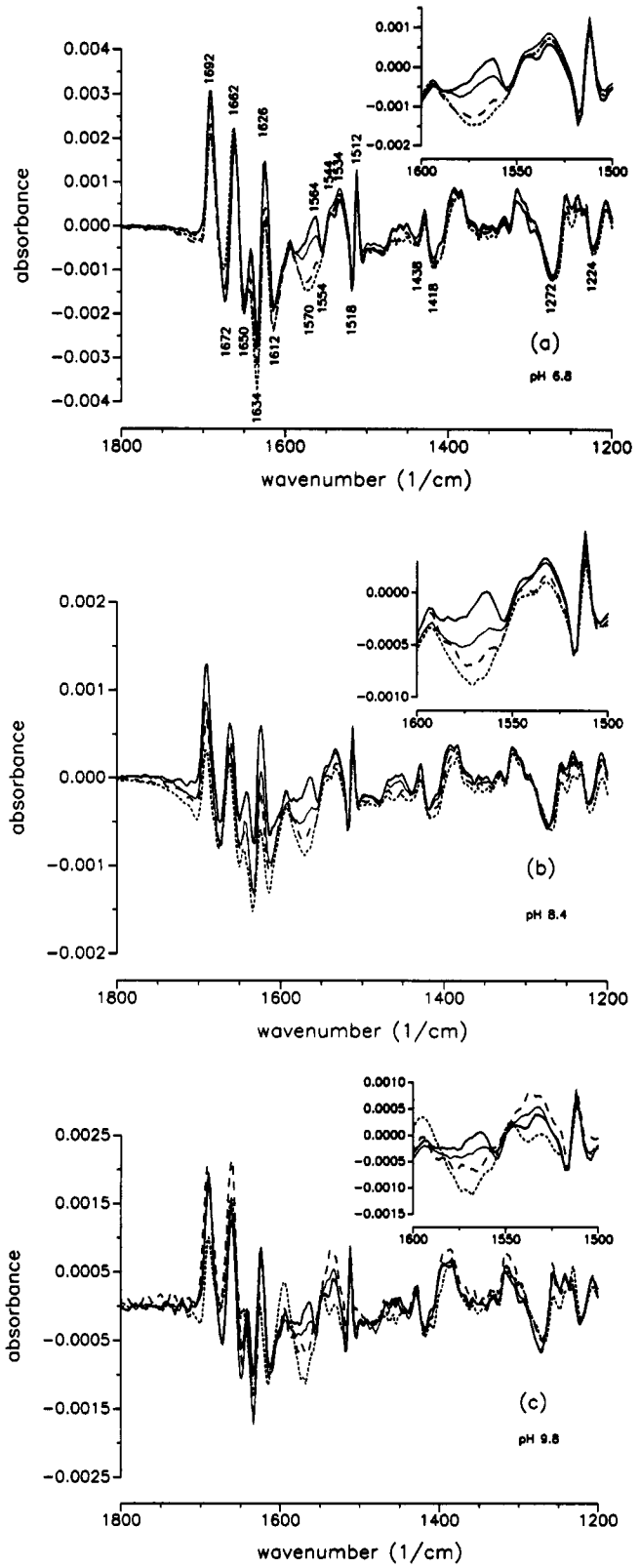

FIGURE 2: Red-ox IR difference spectra of hh cyt c at PyS-SMEs. Effect of temperature and pH. Electrolysis cycles: 100 s at +300/−300 mV. Thick line, 10 °C; thin line, 20 °C; dashed line, 30 °C; dotted line, 40 °C. (a) pH 6.8, (b) pH 8.4, (c) pH 9.8. The insets show the amide-II region in an expanded scale.

cyt c the signals at 1618 and 1602 cm^{-1} to phenylalanine and tyrosine residues.

The amide-I second-derivative IR spectra of both redox states of hh cyt c (Dong et al., 1990, 1992) exhibited major differences in a signal at 1666 cm^{-1}, which was assigned by these authors to β-turns 3_{10}, and no difference in the α-helix content (as judged by the signal at 1657 cm^{-1}) with the redox transition. In contrast to this, our red-ox spectra show a positive difference signal at 1662 cm^{-1}, which suggests a possible contribution of α-helix absorption to the 1666 cm^{-1} band observed by Dong et al. (1990, 1992). The Raman spectrum of hh cyt c shows in the amide-I region a single signal at 1662 cm^{-1} (Liu et al., 1989).

The amide-II spectral region shows four signals of medium intensity at 1564(+), 1554(−), 1544(+), and 1534(+) cm^{-1}. As will be discussed below, this spectral region is the most influenced by changes in temperature. The amide-II band is not as sensitive as the amide-I band to differences in secondary structure (Susi & Byler, 1986). Usually, the amide-II signals arising from different secondary structures appear in the same range of frequencies, leading to extensive overlapping of the signals (Krimm & Bandekar, 1986; Venyaminov & Kalnin, 1990b; Wanthyghem et al., 1990).

We tentatively assign the 1564(+) cm^{-1} signal to β-turns, the 1554(−) cm^{-1} signal to parallel β-sheet structures, the 1544(+) cm^{-1} signal to β-turn 3_{10} segments, and the 1534(+) cm^{-1} signal to antiparallel β-sheet structures (Krimm & Bandekar, 1986). A comparison between the red-ox spectra of cytochromes c from different species (Moss et al., 1990) shows that the signal at 1544(+) cm^{-1} appears only in the hh cyt c spectrum. It has been suggested that a NH_3^+ deformation mode of lysine-60 could be responsible of this signal. The same authors attribute the difference signal at 1564(+)/1554(−) cm^{-1} to the antisymmetric stretching mode of an ionized heme propionate. Kitagawa et al. (1975) have assigned the Raman signals of hh cyt c at 1561 and 1545 cm^{-1} to the C–N stretching mode (amide-II). Liu et al. (1989), however, found the hh cyt c Raman amide-II signal at 1555 cm^{-1}.

The very sharp difference signal at 1518(−)/1512(+) cm^{-1} is typical for the phenol group vibration of tyrosine (Venyaminov & Kalnin, 1990a; Ruegg et al., 1975; Goormaghtigh et al., 1990). The spectral region between 1430 and 1480 cm^{-1} may include signals arising from CH_2 and CH_3 bending modes of amino acid side chains (Susi & Byler, 1983). The signals at 1272(−) and 1224(−) cm^{-1} could have contributions arising from amide-III modes of antiparallel pleated β-sheets and β-turns (II) (Krimm & Bandekar, 1986). A contribution from the $C–O^-$ group stretching vibration of tyrosine could be expected in the 1272 cm^{-1} band (Venyaminov & Kalnin, 1990a). Tyrosine and phenylalanine are also thought to be responsible for a Raman signal at 1210 cm^{-1} (Liu et al., 1989).

Temperature and pH Effect in red-ox Spectra of hh cyt c at PyS-SME. Figure 2a shows a series of red-ox spectra of hh cyt c obtained with the PyS-SME at pH 6.8 and different temperatures in the range 10–40 °C.

At pH 6.8 (Figure 2a), raising the temperature leads to a progressive decrease of the amplitude of the signals at 1692(+) and 1672(−) cm^{-1}. The negative signal at 1650 cm^{-1} becomes influenced by the apparent increase in the amplitude of the siganl at 1634(+) cm^{-1} [the amplitude of the difference signal 1634(−)/1626(+), however, remains constant]. In the amide-II region, the temperature increase leads to the disappearance of the difference signal at 1564(+)/1554(−) cm^{-1}. For temperatures higher than 30 °C, the positive signal at 1564 cm^{-1} disappears and the negative signal at 1554 cm^{-1} becomes overlapped by a broad negative band centered at 1570 cm^{-1}. At the same time, the positive signal at 1544 cm^{-1} becomes less defined, appearing as a shoulder. As a further effect of temperature, a slight shift of 2 cm^{-1} to lower wavenumbers of the band at 1272(−) cm^{-1} is also observed. As it is shown in the inset of Figure 2a, these changes proceed continuously with the temperature increase.

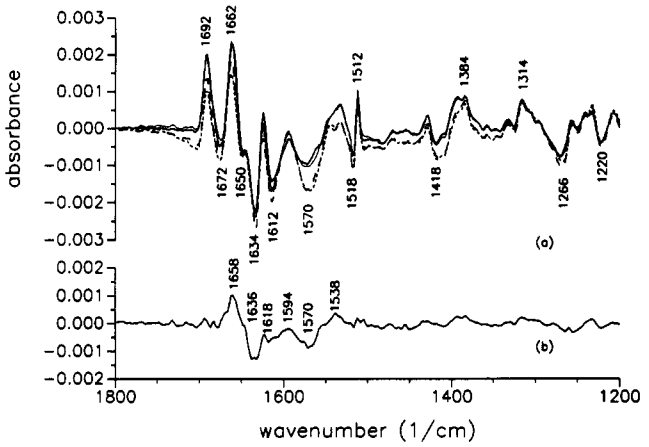

FIGURE 3: (a) Red-ox IR difference spectrum of the same sample as in Figure 2c after recooling and further reheating. Conditions as in Figure 2c. Thick line, 10 °C; thin line, 20 °C; dashed line, 30 °C; dotted line, 40 °C. (b) Subtraction spectrum: 3a (thick line) minus 2c (thick line).

Figure 2b shows an analogous series of spectra recorded at pH 8.4. Comparing the spectrum recorded at 10 °C with the one at pH 6.8 at the same temperature (Figure 2, parts a and b, thick line), the relative amplitude of the positive signal at 1662 cm^{-1} is lower at pH 8.4. The temperature effect is similar at both pH values, although it seems that the broad negative band centered at 1570 cm^{-1} already evolves at lower temperatures at pH 8.4. Indeed, at 20 °C the 1564(+) cm^{-1} signal has almost disappeared (inset Figure 2b). Increasing the temperature leads to a broadening of the negative band at 1418 cm^{-1} and a shift to lower wavenumbers of the 1272(–) cm^{-1} band.

Figure 2c shows a series of spectra recorded at pH 9.8. In the amide-I region, a progressive increase in the amplitude of the signals at 1662(+) and 1634(–) cm^{-1} is observed from starting at low temperatures. The changes in the amide-II region in the range of temperatures from 10 to 30 °C is similar as for pH 6.8 and pH 8.4. However, dramatical changes are detected in the whole spectral range when the temperature is raised to 40 °C. The decrease of the 1692(+) cm^{-1} signal to about 50% of its amplitude at 10 °C is coupled to a large increase of the 1662(+) cm^{-1} signal. The 1550(–) cm^{-1} signal disappears almost completely, and a positive signal at 1594 cm^{-1} appears. The amide-II region shows a broad band centered at 1570(–) cm^{-1}, and a large shift of 6 cm^{-1} toward lower wavenumbers of the 1272(–) cm^{-1} band is observed.

Figure 3a shows a second series of redox-induced difference spectra recorded with the same sample after recooling. It was not possible to recover the initial difference spectrum, and no further changes with the temperature increase were detected. The same treatment applied to a sample at pH 6.8 resulted in the complete recovery of the initial spectrum (data not shown). When comparing with the neutral spectrum, the alkaline IR red-ox spectrum shows a different distribution of amplitudes of the amide-I difference signals. The sum of these amplitudes, however, corresponds to approximately 8% of the absolute amide-I absorbance, which is in agreement with a more opened conformation of ferricytochrome *c* in the alkaline state.

Figure 3b shows a double-difference spectrum obtained by subtraction of the final difference spectrum at 10 °C and the initial difference spectrum at the same temperature. The subtraction shows a main positive signal at 1658 cm^{-1}. At this frequency, the peptide C=O stretching mode arising from the α-helical segments of hh cyt *c* is expected (Dong et al., 1990, 1992). The main negative signal appears at 1636 cm^{-1} and is typically assigned to antiparallel pleated β-sheet structures. This double-difference spectrum shows also some signals of weak intensity at 1538(+), 1618(–), 1594(+), and 1570(–) cm^{-1}. A subtraction of the red-ox difference spectra obtained with the PyS-SME at pH 6.8 at 40 and 10 °C shows no signal at 1658 cm^{-1}; instead, the main difference signal appears at 1666(+)/1636(–) and 1624(–) cm^{-1}, and some signals of weaker intensity at 1690(+), 1596(+), and 1566(–) cm^{-1} (data not shown).

Table I: Conditions of Electrolysis for hh cyt *c* at Different Surface-Modified Electrodes[a]

electrode	pH	reduction potential/time	oxidation potential/time
PyS	6.8[b]	–300 mV/100 s	+300 mV/100 s
PyS	8.4	–300 mV/100 s	+300 mV/100 s
PyS	9.8	–400 mV/300 s	+400 mV/100 s
Cys	6.8[a]	–300 mV/200 s	+300 mV/200 s
Cys	8.4	–300 mV/100 s	+300 mV/100 s
Cys	9.8	–400 mV/100 s	+400 mV/100 s
HPrS	6.8	–300 mV/200 s	+300 mV/100 s
HPrS	8.4	–300 mV/100 s	+300 mV/150 s
HPrS	9.8	–400 mV/100 s	+300 mV/100 s
MB	6.8	–500 mV/200 s	+500 mV/200 s
MB	6.8[c]	–500 mV/300 s	+500 mV/900 s

[a] The sample concentration was approximately 5 mM except where noted. [b] 10 mM. [c] 15 mM.

Along this series of experiments, some differences in the electrochemical reaction are observed (a summary of the conditions of electrolysis used for each experiment is shown in Table I). A decrease of the reduction rate is observed at alkaline pHs. Whereas at pH 6.8 the reaction rates of both reduction and oxidation processes are similar, at pH 8.4 the reduction process becomes slightly slower than the oxidation and at pH 9.8 the reduction rate is threefold slower than the oxidation. However, even at these conditions, it is possible to obtain a "mirror image" ox-red difference spectrum.

Effect of Electrode Surface in Electrochemically Induced Conformational Change of hh cyt c. Figure 4, parts a, b, and c, shows a series of red-ox difference spectra at three different pH values obtained with the Cys-SME. The spectrum recorded at pH 6.8 and 10 °C (Figure 4a, thick line) shows no significant differences with respect to the one obtained with the PyS-SME under the same pH and temperature conditions (Figure 2a, thick line). However, with the Cys-SME, the temperature effect is much weaker. The spectral changes observed are similar to those described for PyS-SME, but they only become apparent once the temperature is raised to 40 °C. At pH values of 6.8 and 8.4, the spectra recorded at 40 °C (Figure 4, parts a and b, dotted line) still show the 1554(–) cm^{-1}. The negative broad band centered at 1570 cm^{-1} in the case of PyS-SMEs now appears splitted, giving rise to two negative signals at 1579 and 1566 cm^{-1}.

A characteristic feature of the Cys-SMEs is the loss of stability at 40 °C which is coupled with a large decrease in the oxidation rate. At temperatures below 40 °C, the electrochemical oxidation and reduction of hh cyt *c* at the Cys-SMEs is slower than at the PyS-SMEs. Even though a loss of the protein reducibility with the pH is detected, the oxidation was slower in every case than the reduction.

At pH 9.8 and 40 °C, it is not possible to obtain red-ox IR difference spectra due to the high unstability of the electrodes. At 30 °C (Figure 4c, dotted line), the only spectral changes are the disappearance of the 1554(–) cm^{-1} signal and a slight shift of the 1272(–) cm^{-1} band toward lower wavenumbers.

In contrast to the Cys-SMEs, the HPrS-SMEs at pH 6.8 are very stable even at 40 °C. The spectral changes (Figure 5a) occur at 40 °C and are similar as for Cys- and PyS-SMEs. The 1554(–) cm^{-1} signal, however, remains throughout the

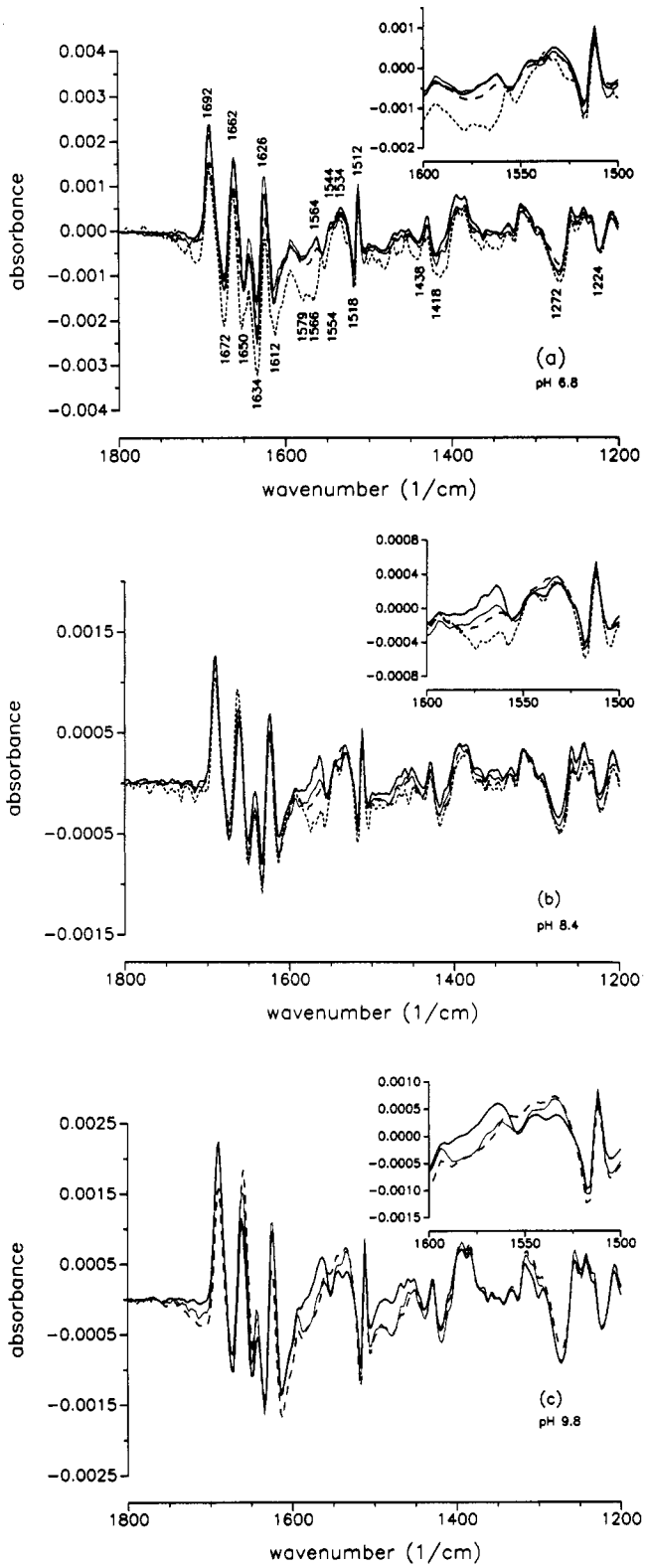

FIGURE 4: Red-ox IR difference spectra of hh cyt *c* at Cys-SMEs. Effect of temperature and pH. Thick line, 10 °C; thin line, 20 °C; dashed line, 30 °C; dotted line, 40 °C. (a) pH 6.8; electrolysis cycles, 200 s at +300/−300 mV. (b) pH 8.4; electrolysis cycles, 100 s at +300/−300 mV. (c) pH 9.8; electrolysis cycles, 100 s at +400/−400 mV. Insets show the amide-II region in an expanded scale.

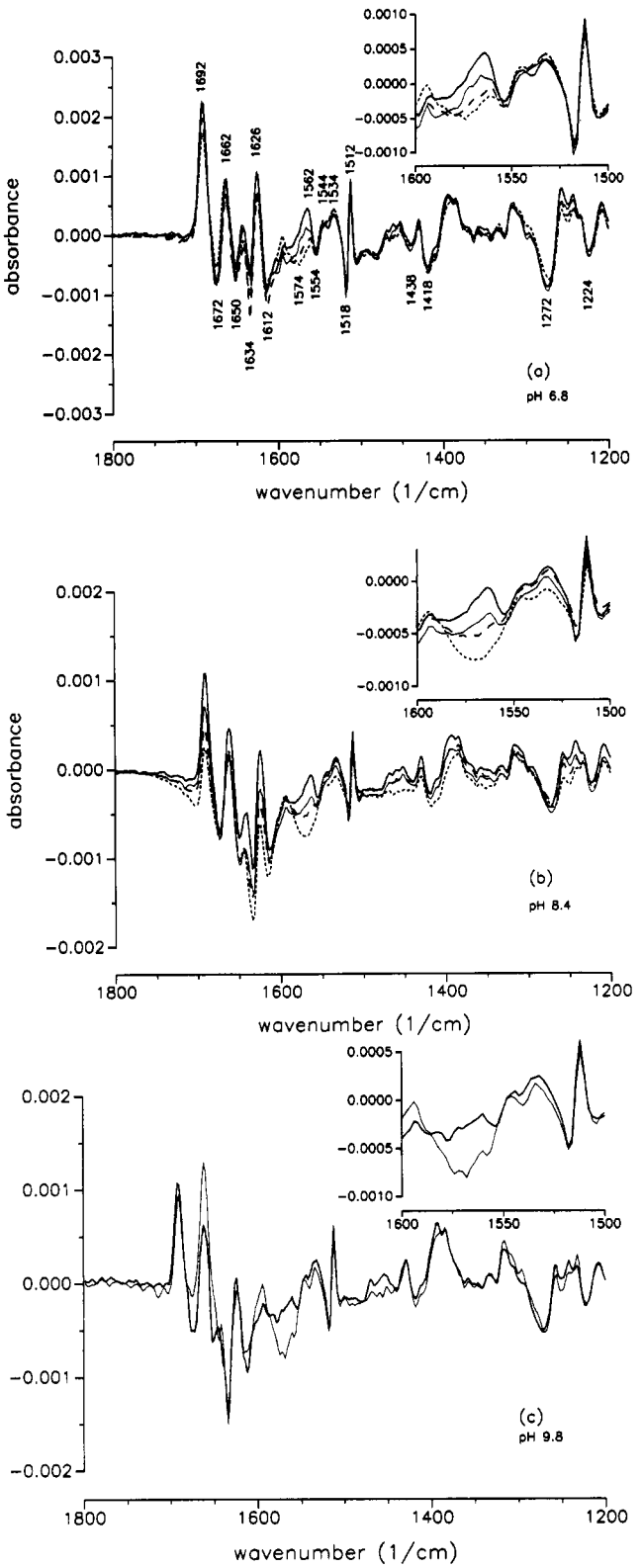

FIGURE 5: Red-ox IR difference spectra of hh cyt *c* at the HPrS-SMEs. Effect of temperature and pH. Thick line, 10 °C; thin line, 20 °C; dashed line, 30 °C; dotted line, 40 °C. (a) pH 6.8; electrolysis cycles, 100 s at +300/−300 mV. (b) pH 8.4; electrolysis cycles, 100 s at +300/−300 mV. (c) pH 9.8; electrolysis cycles, 100 s at +400/−400 mV. Insets show the amide-II region in an expanded scale.

whole range of temperatures. A slight decrease of the amplitude of the 1692(+) cm^{-1} signal is coupled to the temperature increase. At pH 8.4 (Figure 5b), the temperature effect becomes as apparent as for the PyS-SMEs. At pH 9.8 (Figure 5c), the temperature effect is already observed at lower temperatures, and the "alkaline" red-ox spectrum was obtained at 20 °C. Unfortunately, at this pH the electrode is very unstable, leading to the irreversible reduction of the protein. The electrochemical reactions become slower in both directions with the pH increase.

Figure 6a shows a series of red-ox difference spectra obtained at pH 6.8 with a MB-SME. In this case, no effect of temperature is observed. Unfortunately, the large overpo-

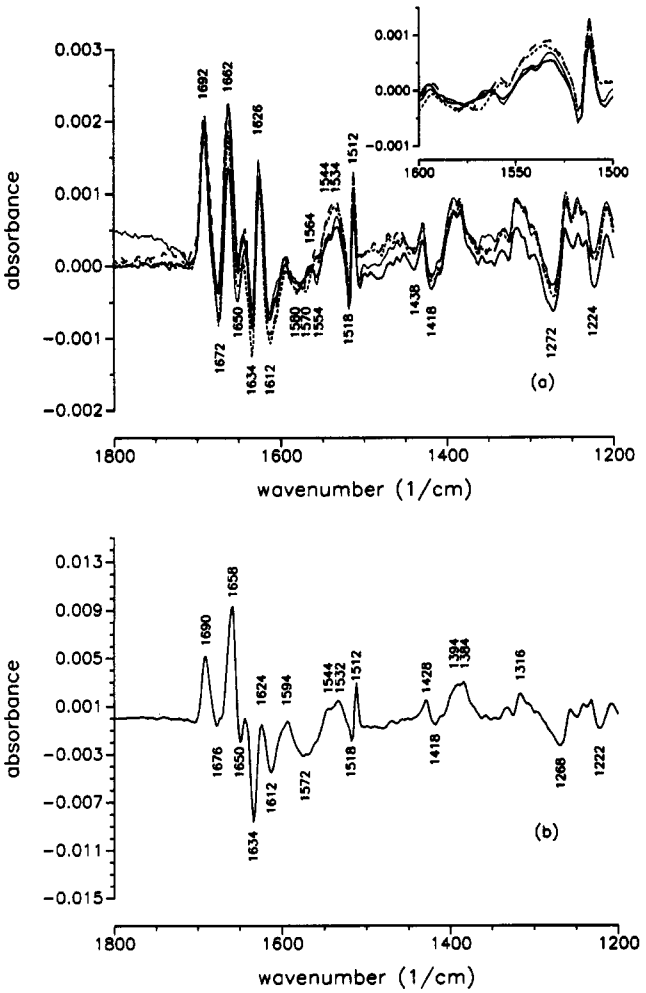

FIGURE 6: Red-ox IR difference spectra of hh cyt *c* at the MB-SMEs at pH 6.8. (a) temperature effect; 5 mM cyt *c*; electrolysis cycles, 200 s at +500/−500 mV. Thick line, 10 °C; thin line, 20 °C, dashed line, 30 °C; dotted line, 40 °C. Inset shows the amide-II region in an expanded scale. (b) 15 mM cyt *c* at 10 °C. Electrolysis cycles, 15 min at +500 mV/5 min at −500 mV.

tentials required to obtain the oxidation/reduction of the protein (+500/−500 mV) do not allow us to perform measurements at higher pH with this electrode. However, when the sample concentration was increased threefold at the same conditions of pH and temperature (Figure 6b), a red-ox spectrum was obtained which strongly resembles the one obtained at pH 9.8 after heating with the PyS-SME. The relative amplitude of the main amide-I difference signal becomes much stronger, as would be expected. There are shifts in the position of some signals, the largest ones corresponding to the 1662 cm^{-1} signal which shifts to 1658 cm^{-1} and the 1272 cm^{-1} band which moves to 1268 cm^{-1}. It is remarkable that the double-difference spectrum shown in Figure 2b also shows the main difference signal at 1658(+)/1636(−) cm^{-1}. The signals at 1690(+) and 1650(−) cm^{-1} and the difference signal at 1518(−)/1512(+) cm^{-1} apparently become much weaker, and the broad band at 1572(−) cm^{-1} becomes much stronger. As for the measurements at pH 9.8 with the PyS-SME, the "mirror image" red-ox difference spectra can be obtained (data not shown), although the oxidation at the MB-SMEs is about threefold slower than the reduction under these conditions.

DISCUSSION

The electrochemically induced red-ox IR difference spectra reflect the entire changes of vibrational modes associated with the redox transition. In Raman spectra, oxidation-state marker bands of the heme have been characterized (Spiro & Li, 1988). In addition, protein bands characteristic for different protein conformations have been detected by UV resonance Raman spectroscopy (Copeland & Spiro, 1985). We would like to emphasize that in the IR difference spectra presented here, bands from the heme, from peripheral heme groups such as the propionates, from amino acid side-chain groups lining up the heme pocket or forming the surface which directs toward the redox partner, and from the polypeptide backbone of the entire molecule can be expected. IR difference signals can arise from protein conformational changes, either affecting the main polypeptide chain or only amino acid side-chain geometries. Furthermore, we would expect changes of local electric field or side group protonation in the protein to cause shifts and changes of intensity of IR bands.

Electrochemically Induced Conformational Change in hh cyt c. A controversy has arisen on the conformational change inherent to the redox transition of cytochrome *c*. According to X-ray crystallography, the redox transition does not involve large changes in the structure of the polypeptide backbone. This change has been described as a concerted movement arising from adjustments to the heme structure, large movements of the internal water molecules, and changes in the thermal parameters of some polypeptide segments (Takano & Dickerson, 1981a,b; Berghuis & Brayer, 1992). The largest movements are centered in the pyrrole-A-heme propionate, the internal water molecule Wat-166, Met-80, and the polypeptide segments surrounding these residues, beside the heme ring itself. Wat-166 and Met-80 are bound through a network of hydrogen bonds involving the residues Asn-52, Tyr-67, Thr-78, and Phe-82 (Berghuis & Brayer, 1992).

The heme group in cyt *c* is covalently bound to the polypeptide backbone by two thioether linkages from Cys-14 and Cys-17, both residues included in a short β-turn 3_{10} segment. Tyr-67 is also in a β-turn 3_{10} segment which connects two α-helices. Asn-52 is included in an α-helix, and Met-80 and Phe-82 are in a region of unordered structure (Bushnell et al., 1990). Liu et al. (1989) have found that the region surrounding Trp-59 became more accessible to the solvent in the oxidized state. According to Bushnell et al. (1990), this residue belongs to a very short β-sheet segment. The same was observed from oxidation-state-dependent differences in the NMR chemical shifts of residues included in the 50–60 segment, which contains an α-helix (Feng & Englander, 1990).

According to the hh cyt *c* secondary structure proposed by Bushnell et al. (1990), hh cyt *c* has only two short segments of β-sheet structures. This seems to disagree with our observations from the red-ox IR difference spectra presented here and with the hh cyt *c* second-derivative amide-I IR spectra of Dong et al. (1992), who have attributed several large IR signals to β-sheet structures, and with the estimation of secondary structure from the IR amide-I band of Kalnin et al. (1990). Dickerson et al., (1971), in an earlier crystallographic study, have described the molecule of hh cyt *c* as containing β-sheet extended chains at the right and the left side of the heme group, containing the residues Cys-14, Cys-17, His-18, and Met-80. Among the four tyrosines and four phenylalanines of hh cyt *c*, only Tyr-67, Tyr-48, and Phe-82 are thought to be involved in the redox process (Takano & Dickerson, 1981b).

Temperature and pH Effect on red-ox Difference Spectra of hh cyt c at PyS-SMEs. The hh cyt *c* thermal denaturation proceeds reversibly as a two-step process with a transition temperature (T_{tr}) for the first transition around 50 °C (Santucci et al., 1989). This step reflects a loosening of the

structure of the heme crevice, with a partial disruption of the hydrophobic environment and, thus, the exposing of some peptides to the solvent. The first thermal transition gives rise to the same intermediate states as those obtained by partial denaturation with 4.5 M urea at neutral pH (Myer et al., 1980). Angström et al. (1982) have found that in the thermal denaturation process at neutral pH there is a transition at 40 °C to the alkaline form of ferricytochrome c, in which the Met-80-S-Fe bond is broken followed by a substitution of Met-80 by another strong-field ligand, probably a lysine. Since strong evidences against Lys-72, -73, or -79 as ligands have been found (Bosshard, 1981), Lys-13, -86, or -87 have been suggested as potential heme ligands (Gadsby et al., 1987). It should be noted that, in any case, this ligand exchange would imply a movement of an α-helix. The temperature increase leads to a decrease in the apparent pK_a of the alkaline transition. This transition is also responsible for the sharp biphasic behavior observed in the temperature dependence of the redox potentials of the hh cyt c, with an apparent pK_a of 9.8 at 20 °C (Ikeshoji et al., 1989). The same authors found that the thermal transition is reversible and has a T_{tr} which shifts from 50 °C at pH 6.8 to 25 °C at pH 9.2.

We have found that raising the pH to 9.8 leads to the same spectral changes as those observed by heating at neutral pH. The major spectral changes arising from temperature increase are mainly affecting negative bands in the difference spectra; in our convention, these changes are thus associated with changes in the oxidized state of hh cyt c. The spectra show an evolution to the alkaline state at lower temperature with increasing pH, which is in agreement with a diminishing of the pK_a of the alkaline transition at high temperatures. At pH 9.8 the alkaline spectrum of hh cyt c was only obtained after raising the temperature to 40 °C. It is not possible to recover the neutral spectra after recooling, and no further spectral changes after a second cycle of heating were observed. This suggests that indeed the conformational change associated to the alkaline transition is slow and favored at high temperatures.

The spectral changes coupled to the reaching of the alkaline transition are consistent with a rearrangement of the polypeptide backbone which affects α-helical and β-sheet segments. The shift of the tyrosine band at 1272 cm^{-1} toward lower wavenumbers by 6 cm^{-1} indicates the ionization of the hydroxyl groups after the alkaline transition (Venyaminov & Kalnin, 1990a). The negative band at 1570 cm^{-1} could arise from a NH_3^+ deformation mode of the lysines surrounding the heme crevice. A more opened configuration of the heme crevice similar to that found by Liu et al. (1989) for hh cyt c at low ionic strength would agree with the spectral changes observed. The shift of only one of the tyrosine signals may reflect that only Tyr-48 is now more exposed to the solvent and that Tyr-67 remains deeply buried in the heme pocket. The loosening of the heme crevice structure may lead to the same effect observed at low ionic strength: the movement of the α-helix 49–55 with the disruption of the hydrogen bond between Tyr-48 and the heme propionate.

Effect of Electrode Surface Modification on Conformation of hh Ferricytochrome c. The red-ox spectra of hh cyt c either in the neutral or the alkaline state are identical and independent on the kind of electrode used. However, we have seen large differences in the conditions at which the alkaline form of the spectra is reached, depending on the nature of the electrode surface. Whereas with the PyS-SMEs the thermally induced transition to the alkaline form of the spectra happened in the whole range of pH tested, the spectra obtained with Cys-SMEs always show the neutral form. With the HPrS-SMEs an intermediate behavior was observed, since it was necessary to raise the pH to 8.4 to obtain the thermally induced alkaline transition. However, the latter electrodes favored the alkaline transition at pH 9.8. These phenomena can be interpreted in terms of stabilization–destabilization of the hh cyt c structure arising from the specific interactions between the protein and the molecules of promoter covering the electrode surface.

PyS is adsorbed as an array of pyridyl groups directed away from the electrode surface. The interaction with cyt c is achieved through weak hydrogen bonds between the nitrogens of the pyridyl rings and the positively charged lysines located in the protein surface (Allen et al., 1984). In the case of Cys and HPrS-SMEs, the interaction may be stronger through a mixture of hydrogen bonds and electrostatic interactions with the charged COO^- and NH_3^+ groups of the promoters (Di Gleria et al., 1986; Hill & Lawrance, 1989). A fully negatively charged covered surface would favor an opened conformation of the protein as it has been observed in hh cyt c bound to negatively charged phospholipid membranes (Muga et al., 1991). This has also been observed with hh cyt c bound to vesicles and inverted micelles (Hildebrandt & Stockburger, 1989b), absorbed on colloidal silver particles (Hildebrandt & Stockburger, 1986a), or on gold electrodes (Hinnen & Niki, 1989). It has been shown that hh cyt c irreversibly adsorbed on a gold-PyS electrode preserves its native conformation, whereas on an electrode partially covered with dipyridyl the protein adsorbs in an opened conformation (Hinnen & Niki, 1989). The interaction between PyS and hh cyt c has also been studied in solution phase (Sagara et al., 1991). These authors have found that the binding of PyS to cyt c does not induce the structural change that shifts the formal potential toward more negative values.

What we have observed agrees with a stabilization of a "closed" structure of hh cyt c at the Cys-SMEs in the whole range of pH studied and at the HPrS and MB-SMEs at neutral pH, suggesting a weaker interaction of the promoter and the protein in the PyS-SMEs. The acceleration of the transition at pH 9.8, with the HPrS-SMEs observed, agrees with a loosening of the protein structure due to an excess of negative charges at the electrode surface at this pH. The stability of the electrodes can be easily monitored by the kinetics of the oxidation process (data not shown). A bare metallic electrode leads to the irreversible reduction process with adsorption of the protein on the metallic surface and a complete loosening of the overall tertiary structure. The case of MB-SMEs with high protein concentrations could be explained by the partial covering of the electrodes, which would lead to a partial unfolding of the protein at the electrode surface.

CONCLUSIONS

The redox-induced IR difference spectra of hh cyt c demonstrate that the combination of protein electrochemistry and IR spectroscopy provides a considerable potential for the study of functionally related protein conformational changes. With electrochemical techniques at surface-modified electrodes avoiding redox mediators, (which would, at higher concentrations, interfere with their IR absorbance), quantitative and reversible redox reactions can be achieved. This allows us to obtain IR difference bands directly related with the redox process in the protein.

The red-ox IR difference spectra of hh cyt c shown in this work not only reflect the conformational change arising from the redox transition but also show differences depending on the initial state of the protein before the redox reaction. The spectral changes observed with changes in temperature and pH show a transition between two different states of ferri-

cytochrome *c* from its native "closed" state to an "opened" state arising from the loosening of the heme crevice structure. Moreover, the red-ox spectra show clearly that the thermally and pH-induced processes give rise to essentially the same species, which is the alkaline state of ferricytochrome *c*.

We have also shown in this work that the nature of the electrode surface must be taken into account in these kinds of studies. The specific interactions between the protein and the molecules of promoter adsorbed onto the electrode surface may be responsible for a stabilization/destabilization of the native structure of the protein and, thus, masking the alkaline transition.

Although the analysis of the FTIR difference spectra is far from being complete, this technique can be complementary to high-resolution structure analysis. Since neither crystalline nor highly purified samples are required for IR difference spectroscopy, the molecular mechanisms accompanying the redox transition can be studied at conditions close to the native reactions. The information from redox-induced FTIR difference spectra thus complements and supplements the structural information obtained, for example, from the crystalline state, and may lead to a consistent picture of how a given structure leads to a specific function.

ACKNOWLEDGMENT

The authors would like to thank Dr. Víctor M. Fernández, Instituto de Catálisis y Petroleoquímica, Madrid, and Prof. W. Kreutz, Institut für Biophysik, for encouraging support.

REFERENCES

Allen, P. M., Hill, H. A. O., & Walton, N. J. (1984) *J. Electroanal. Chem. 178*, 69–86.
Angström, J., Moore, G. R., & Williams, R. J. P. (1982) *Biochim. Biophys. Acta 703*, 87–94.
Arrondo, J. L. R., Young, N. M.; & Mantsch, H. H. (1988) *Biochim. Biophys. Acta 952*, 261–268.
Baymann, F., Moss, D., & Mäntele, W. (1991) *Anal. Biochem. 199*, 269–274.
Berghuis, A. M., & Brayer, G. D. (1992) *J. Mol. Biol. 223*, 959–976.
Bosshard, H. R. (1981) *J. Mol. Biol. 153*, 1125–1149.
Bushnell, G. W., Louie, G. V., & Brayer, G. D. (1990) *J. Mol. Biol. 214*, 585–595.
Casal, H. L., Kohler, U., & Mantsch, H. H. (1988) *Biochim. Biophys. Acta 957*, 11–20.
Copeland, R. A., & Spiro, T. G. (1985) *Biochemistry 24*, 4960–4968.
Dickerson, R. E., Takano, T., Eisenberg, D., Kallai, O. B., Samson, L., Cooper, A., & Margoliash, E. (1971) *J. Biol. Chem. 246*, 1511–1535.
Di Gleria, K., Hill, H. A. O., Lowe, V. J., & Page, D. J. (1986) *J. Electroanal. Chem. 213*, 333–338.
Dong, A., Huang, P., & Caughey, W. S. (1990) *Biochemistry 29*, 3303–3308.
Dong, A., Huang, P., & Caughey, W. S. (1992) *Biochemistry 31*, 182–189.
Feng, Y., & Englander, S. W. (1990) *Biochemistry 29*, 3494–3504.
Feng, Y., Roder, H., & Englander, S. W. (1990) *Biochemistry 29*, 3505–3509.
Gadsby, P. M. A., Peterson, J., Foote, N., Greenwood, C., & Thomson, A. J. (1987) *Biochem. J. 246*, 43–54.
Goormaghtigh, E., Cabiaux, V., & Ruyschaert, J. M. (1990) *Eur. J. Biochem. 193*, 409–420.
Hildebrandt, P., & Stockburger, M. (1986) *J. Phys. Chem. 90*, 6017–6024.
Hildebrandt, P., & Stockburger, M. (1989a) *Biochemistry 28*, 6710–6721.
Hildebrandt, P., & Stockburger, M. (1989b) *Biochemistry 28*, 6722–6728.
Hill, H. A. O., & Lawrance, G. A. (1989) *J. Electroanal. Chem. 270*, 309–318.
Hinnen, C., & Niki, K. (1989) *J. Electroanal. Chem. 264*, 157–165.
Ikeshoji, T., Taniguchi, I., & Hawkridge, F. M. (1989) *J. Electroanal. Chem. 270*, 297–308.
Kalnin, N. N., Baikalov, L. A., & Venyaminov, S. Y. (1990) *Biopolymers 30*, 1273–1280.
Kitagawa, T., Kyogoyu, Y., Izuka, T., Ikeda-Saito, M., & Yamanaka, T. (1975) *J. Biochem. 78*, 719–728.
Krimm, S., & Bandekar, J. (1986) *Adv. Prot. Chem. 38*, 181–367.
Liu, G., Grygon, C. A., & Spiro, T. G. (1989) *Biochemistry 28*, 5046–5050.
Moss, D., Nabedryk, E., Breton, J., & Mäntele, W. (1990) *Eur. J. Biochem. 187*, 565–572.
Muga, A., Mantsch, H. H., & Surewicz, W. K. (1991) *Biochemistry 30*, 7219–7224.
Myer, Y. P., MacDonald, L. H., Verma, B. C., & Pande, A. (1980) *Biochemistry 19*, 199–207.
Poulos, T. L., & Kraut, J. (1980) *J. Biol. Chem. 255*, 10322–10330.
Ruegg, M., Metzger, V., & Susi, H. (1975) *Biopolymers 14*, 1465–1470.
Sagara, T., Satake, I., Murakami, H., Akutsu, H., & Niki, K. (1991) *J. Electroanal. Chem. 301*, 285–290.
Salemme, F. R. (1976) *J. Mol. Biol. 102*, 563–568.
Salemme, F. R., Kraut, J., & Kamen, M. D. (1973) *J. Biol. Chem. 248*, 7701–7716.
Santucci, R., Giartosio, A., & Ascoli, F. (1989) *Arch. Biochem. Biophys. 275*, 496–504.
Schlereth, D. D., & Mäntele, W. (1992) *Biochemistry 31*, 7494–7502.
Spiro, T. G., & Li, X.-Y. (1988) in *Biological Applications of Raman Spectroscopy* (Spiro, T. G., Ed.) Vol. 3, pp 1–38, Wiley, New York.
Stellwagen, E. (1978) *Nature 275*, 73–74.
Surewicz, W. K., Szabo, A., & Mantsch, H. H. (1987) *Eur. J. Biochem. 167*, 519–523.
Susi, H., & Byler, D. M. (1983) *Biochem. Biophys. Res. Commun. 115*, 391–393.
Susi, H., & Byler, D. M. (1986) *Methods Enzymol. 130* (13), 290–311.
Susi, H., & Byler, D. M. (1987) *Arch. Biochem. Biophys. 258*, 465–469.
Takano, T., & Dickerson, R. E. (1981a) *J. Mol. Biol. 153*, 79–94.
Takano, T., & Dickerson, R. E. (1981b) *J. Mol. Biol. 153*, 95–115.
Taniguchi, I., Toyosawa, K., Yamaguchi, H., & Yasukuochi, K. (1982a) *J. Chem. Soc. Chem. Commun.*, 1032–1033.
Taniguchi, I., Toyosawa, K., Yamaguchi, H., & Yasukuochi, K. (1982b) *J. Electroanal. Chem. 140*, 187–193.
Venyaminov, S. Y., & Kalnin, N. N. (1990a) *Biopolymers 30*, 1243–1257.
Venyaminov, S. Y., & Kalnin, N. N. (1990b) *Biopolymers 30*, 1259–1271.
Wanthyghem, J., Baron, M. H., Picquart, M., & Lavaille, F. (1990) *Biochemistry 29*, 6600–6609.